

The Correlation of Benzene Production with Soot Yield Determined from Fuel Pyrolyses

R.D. Kern, C.H. Wu, J.N. Yong, K.M. Pamidimukkala and H.J. Singh

Department of Chemistry
University of New Orleans
New Orleans, Louisiana 70148

Introduction

The rate of production of soot in pyrolytic reaction systems has been studied in shock tubes using a variety of non-intrusive analytical techniques; laser extinction (LEX)¹⁻⁶, static analysis of the product distribution from single pulse shock tubes (SPST)⁷⁻⁹, and dynamic analysis of the reflected shock zone by time-of-flight mass spectrometry (TOF)¹⁰. The data reduction process often involves measurement of a changing bulk quantity; e.g., attenuation of a He-Ne laser beam due to absorption by high molecular weight gas phase species and discrete soot particles via LEX or deficiencies in the carbon atom mass balance via SPST or TOF. The concentrations of the various polycyclic hydrocarbons formed in the pre-particle soot chemistry phase are extremely low⁹ and are below the detectability limit of the TOF technique¹⁰ which is about 10^{-10} mol cm^{-3} . The non-detected hydrocarbons constitute the "missing" mass.

The ultimate goal of the work in this area is to write a complete chemical mechanism for soot formation. This formidable task has been attempted for acetylene¹¹. Some 180 species and 600 reactions were considered in an effort to model the soot yield obtained by LEX. Both the calculated and experimental yields were very low (< 1%). Comparison of the calculated results with the measured bulk quantity was obtained by assuming that all species in the model having $MW > 300$ absorbed 632.8 nm radiation. The summation of these high molecular weight concentrations converted to carbon atoms cm^{-3} and divided by the input carbon atom concentration yielded the computed soot yield.

The effort herein is to develop a correlation between a readily observable molecular species whose presence is diagnostic of subsequent soot formation and the bulk observables of laser extinction and mass balance deficiency.

Experimental Techniques Employed

LEX has been utilized behind incident and reflected shock waves during various observation times ranging from 0.5-2.5 ms¹⁻⁶. In order to compare the relative sooting tendencies of fuels, a total carbon atom concentration of 2×10^{17} atoms cm^{-3} was chosen for such fuels as ethylbenzene, toluene, benzene, pyridine, allene, 1,3 butadiene, vinylacetylene, and acetylene. The soot yield vs the no-reaction shock zone temperature curves are bell-shaped. Aromatic compounds produced the greatest amount of beam attenuation or soot yield while

acetylene exhibited the least. The early LEX work¹⁻³ reported values for the absolute soot yield on the order of 80 - 90% conversion of aromatic fuels to soot. It was subsequently realized that these values were too high due in part to uncertainty of the literature value for the refractive index of soot and to light absorption by pre-particle species.⁴ It was also known that a significant amount of soot formation occurred in the accompanying cooling wave.^{7,8} For these and other reasons, the ordinate for soot yield plots was taken to be $E(m) \times$ soot yield with the value of $E(m)$ left unspecified pending resolution of the uncertainties.^{4,5} This adjustment cast the LEX results as a measurement of relative rather than absolute soot yields.

The thrust of the mass balance deficiency procedure was to add up all of the carbon containing products detected and subtract from the total carbon atoms in the original fuel. Aromatic compounds showed the greatest deficiencies (with the notable exception of pyridine⁶) and acetylene the least. There was good agreement with regard to the relative sooting tendencies of fuels investigated with LEX and the mass deficiencies obtained by SPST and TOF.

The TOF method offers the advantage of recording the product distribution at selected times during the reaction. Concentration profiles of various observed species are constructed within the m/e range of 12 - 300 during typical observation times of ~ 0.75 ms. The data are fit with computed lines from proposed or known mechanisms. Benzene has been recorded during the pyrolyses of allene¹², 1,2 butadiene¹³, and 1,3 butadiene¹⁴. The profiles have been modeled using the CHEMKIN program^{15,16} with reasonable success.

Results and Discussion

In order to mimic the soot bells determined by LEX, benzene concentrations were modeled for the thermal decompositions of C_3H_4 ¹²; 1,2 C_4H_6 ¹³, 1,3 C_4H_6 ¹⁴, C_4H_4 ¹⁷, C_5H_5N ¹⁸, and C_2H_2 ¹⁹. In each of these pyrolyses investigated by the TOF method, the total carbon atom concentration was approximately 2×10^{17} atoms cm^{-3} . The benzene concentrations were calculated for each of these fuels at 1 ms as a function of no-reaction shock temperature in order to compare with the LEX work. The TOF and LEX results are shown in Figures 1 and 2. Before discussing each fuel individually, we note that the benzene concentration curves are bell shaped, that the relative amounts of benzene formed are in the same general order as the sooting tendencies, and that the benzene maximum for each fuel precedes the respective soot tendency maxima.

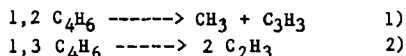
Allene

A 4.3% C_3H_4 -Ne mixture was investigated over the temperature and total pressure range of 1300-2000 K and 0.2-0.5 atm, respectively. TOF analysis revealed that the major products were C_2H_2 , C_4H_2 , CH_4 and C_6H_6 ; lesser amounts of C_2H_4 , C_2H_6 , C_4H_4 , and C_6H_2 were detected. The major product profiles were modeled with an 80 step reaction mechanism. The initial reactions involved the isomerization of allene to propyne²⁰; both isomers decompose to yield $C_3H_3 + H$ ^{21,22}. Benzene was produced via reaction of C_3H_3 with allene and by reaction of

two C_3H_3 radicals. The latter route was suggested by Hurd^{23,24} in which C_3H_3 initially forms $:CH-CH=CH$ via 1,2 H shift followed by cyclization to benzene. Benzene concentrations were calculated at 1 ms for various no-reaction temperatures. The resulting bell shaped curve is displayed in Figure 1 along with its respective LEX soot tendency bell⁵.

1,2 Butadiene

A 3% 1,2 C_4H_6 -Ne mixture was shocked over the ranges 1200-2000 K and 0.17-0.56 atm. The major stable species observed were C_2H_2 , CH_4 , C_2H_4 and C_4H_2 . At intermediate temperatures (around 1500 K), benzene and toluene were recorded. C_2H_2 and C_4H_2 were the only major products at high temperatures. Isomerization of 1,2 to 1,3 C_4H_6 precedes extensive decomposition. The two isomers decompose according to two pathways.



The decomposition of 1,3 C_4H_6 has been studied by laser schlieren densitometry (LS) and TOF¹⁴. The reaction mechanism used to model the various product profiles from 1,3 C_4H_6 was employed as a subset to the mechanism for 1,2 C_4H_6 . Reactions describing the isomerization and other key channels complete the model. Benzene concentrations were calculated at 1 ms and are plotted as a function of temperature in Figure 1. There are no LEX data available for comparison.

1,3 Butadiene

A 3% 1,3 C_4H_6 -Ne mixture was studied over the range comparable to 1,2 C_4H_6 . LS profiles obtained by Professor Kiefer provided conclusive evidence that the main pathway for decomposition was C-C bond rupture to produce two vinyl radicals. A 31 step mechanism modeled the LS profiles and the TOF profiles for 1,3 C_4H_6 , C_2H_2 , C_2H_4 , C_4H_2 and C_6H_6 ¹⁴. The amount of benzene produced was less than that recorded for 1,2 C_4H_6 and for an equivalent amount of C_3H_4 . The latter result is in agreement with the LEX work⁵ which is shown in Figure 1.

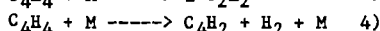
Acetylene

C_2H_2 is the major product in the high temperature thermal decompositions of many hydrocarbons; C_8H_{10} ²⁵, C_7H_8 ²⁶, C_6H_6 ²⁷⁻²⁹, C_5H_5N ¹⁸, C_3H_4 ¹², 1,2¹² and 1,3 C_4H_6 ¹⁴, and C_4H_4 ³⁰. A radical mechanism derived largely from those previously employed by Gardiner³¹ and Kiefer³² was used to model TOF data obtained on a series of C_2H_2 -Ne mixtures, 1-6.2%, over the range 1900-2500 K and 0.3-0.55 atm. The major species modeled were C_2H_2 , C_4H_2 , and C_6H_2 . Minor amounts of C_8H_2 and C_4H_3 were recorded; benzene was not detected. Reactions from the benzene mechanism²⁹ were added to the model and used to calculate the relatively minor amounts of benzene detected in the SPST work by Colket⁹. The results are shown in Figure 3. Although the fit is not completely satisfying, the computed profile is satisfactory for our purpose here; namely, the benzene yield is very low compared to the major species present. Benzene concentrations for an acetylene

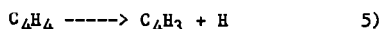
mixture containing 2×10^{17} C atoms cm^{-3} are plotted in Figure 2 along with the corresponding LEX soot bell⁵.

Vinylacetylene

Pyrolysis of C_4H_4 has been studied recently by LS and TOF over the range 1500–2500 K and 0.14–0.56 atm³⁰. Analysis of the LS profiles revealed that the decomposition was characterized by a heat release of ~ 40 kcal mol^{-1} . The LS profiles were all concave upward which ruled out any appreciable chain acceleration reactions. TOF measurements of the major products, C_2H_2 and C_4H_2 disclosed a near constant ratio of $\text{C}_2\text{H}_2/\text{C}_4\text{H}_2 \sim 5$ which was independent of the observation time and temperature. Trace amounts of C_6H_2 were recorded at higher temperatures; C_8H_2 and benzene were not detected. These facts support the proposal that the mechanism is molecular and occurs via the reactions



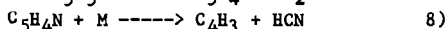
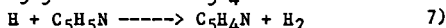
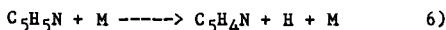
The LS profiles and the TOF profiles were fit with rate constants derived for this two channel dissociation. These conclusions are in conflict with two other shock tube reports that propose a radical mechanism for the pyrolysis in which the first step is C-H bond rupture^{33,34}.



The initiation is followed by a sequence of radical reactions. The benzene concentrations shown in Figure 2 were calculated using rxns 3) and 4) along with the C_2H_2 ¹⁹ and C_6H_6 ²⁹ mechanisms previously mentioned to fit the SPST data in Figure 3.

Pyridine

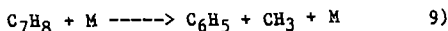
LS and TOF profiles have been recently obtained¹⁸ for the thermal decomposition of $\text{C}_5\text{H}_5\text{N}$ over the range 1700–2200 K and 0.13–0.5 atm. The LS profiles displayed local maxima which is a signature for chain acceleration of the net endothermic rate. The main products were identified by TOF to be HCN, C_2H_2 , and C_4H_2 . A 24 step mechanism was constructed which included the following steps:



Benzene concentrations were calculated in the manner employed for C_4H_4 and are extremely low which is in accord with the LEX result⁶. The near absence of this key building block inhibits polycyclic growth and subsequent soot formation. Intact pyridine rings are not suitable substitutes since polycyclic growth is retarded by the presence of the ring nitrogen.

Temperature Changes

Thermal decompositions are endothermic processes and the system temperature decreases as the reaction progresses. This point is illustrated in Figure 4 in which the soot bell for toluene at 1 ms observation time⁴ is shifted markedly when the system temperature at 1 ms is used to plot the sooting tendency instead of the usual practice which employs the no reaction temperature. The temperatures at 1 ms were calculated using a mechanism from recent LS and TOF work on C₇H₈²⁶ which identifies the major pathway for dissociation as



Temperature decreases for the pyrolyses represented in Figures 1 and 2 at 1 ms are listed in Table 1.

Conclusions

There appears to be sufficient evidence to support the correlation of benzene production and soot tendencies. It does not necessarily follow that the key to soot control is limiting solely those reactions and/or species which promote benzene formation. The pyrolyses considered herein were those of "pure" fuels. Synergistic effects have been reported for fuel mixtures; e.g., a 0.75% C₇H₈ - 0.75% C₅H₅N - Ar mixture produced almost as much soot as an equivalent amount of "pure" toluene, 1.5% C₇H₈ - Ar⁶. Nevertheless, the results herein are consistent with the proposal of relatively low concentrations of soot nuclei which subsequently increase in mass due to surface growth by C₂H₂³⁵.

Acknowledgments

We appreciate the collaboration of Professor Kiefer and his research group and thank the Department of Energy for support under contract DE-FG0585ER/13400.

References

1. Graham, S.C., Homer, J.B. and Rosenfeld, J.L.J., Proc. Roy. Soc. A344(1975) 259.
2. Graham, S.C., Homer, J.B. and Rosenfeld, J.L.J., Proc., 10th Int. Symp. on Shock Tubes and Waves, 1975, p.621.
3. Wang, T.S., Matula, R.A. and Farmer, R.C., 18th Symp. (Int.) on Combustion (1981), 1149.
4. Frenklach, M., Taki, S. and Matula, R.A., Combust. Flame, 49, (1983), 275.
5. Frenklach, M., Taki, S. Durgaprasad, M.B. and Matula, R.A., Combust. Flame, 54, (1983) 81.
6. Rawlins, W.T., Tanzawa, T., Schertzer, S.P., and Kreck, R.H., Final Report submitted to DOE, Contract DEAC2280PC30292, January 1983.
7. Vaughn, S.N., Ph. D. Thesis, Kansas State University, 1980.
8. Vaughn, S.N., Lester, T.W. and Merklin, J.F., Proc., 13th Int. Symp. on Shock Tubes and Waves, 1982, p. 860.
9. Colket, M.B., Proc., 15th Int. Symp. on Shock Tubes and Waves, 1986, p. 311.

10. Kern, R.D., Singh, H.J., Esslinger, M.A. and Winkeler, P.W., 19th Symp. (Int.) on Combustion, 1982, 1351.
11. Frenklach, M., Clary, D.W., Gardiner, W.C., and Stein, S.E., 20th Symp. (Int.) on Combustion, (1984), 887.
12. Wu, C.H. and Kern, R.D., manuscript submitted to J. Phys. Chem.
13. Singh, H.J. and Kern, R.D., work in progress.
14. Kiefer, J.H., Wei, H.C., Kern, R.D. and Wu, C.H., Int. J. Chem. Kinet., 17, (1985) 225.
15. Kee, R.J., Miller, J.A. and Jefferson, T.H., CHEMKIN: A General Purpose, Problem Independent Transportable, Fortran Chemical Kinetics Code Package, Sandia National Laboratories, SAND 80-8003, 1980.
16. Hindmarsh, A.C., LSODE Livermore Solver for Ordinary Differential Equations, Lawrence Livermore Laboratory, 1980.
17. Kiefer, J.H., Mitchell, K.I., Kern, R.D., and Yong, J.N., manuscript submitted to J. Phys. Chem.
18. Kern, R.D., Yong, J.N., Kiefer, J.H., and Shah, J.N., paper to be presented at the 16th Int. Symp. on Shock Tubes and Waves, 1987.
19. Wu, C.H. and Kern, R.D., manuscript submitted to Int. J. Chem Kinet.
20. Kakumoto, T., Ushirogouchi, T., Saito, K., Isamura, A., J. Phys. Chem., 91, (1987), 183.
21. Lifshitz, A., Frenklach, M., Burcat, A., J. Phys. Chem., 79, (1975), 1148.
22. Lifshitz, A., Frenklach, M., Burcat, A., J. Phys. Chem., 80, (1976), 2437.
23. Hurd, C.D., Macon, A.R., Simon, J.I., Levetan, R.V., J. Am. Chem. Soc., 84, (1962), 4509.
24. Hurd, C.D., Macon, A.R., J. Am. Chem. Soc., 84, (1962), 4524.
25. Pamidimukkala, K.M. and Kern, R.D., Int. J. Chem. Kinet., 18, (1986), 1341.
26. Pamidimukkala, K.M., Kern, R.D., Patel, M.R., Wei, H.C. and Kiefer, J.H., J. Phys. Chem., 91, (1987), 2148.
27. Singh, H.J. and Kern, R.D., Combust. Flame, 54, (1983), 49.
28. Kern, R.D., Wu, C.H., Skinner, G.B., Rao, V.S., Kiefer, J.H., Towers, J.A., and Mizerka, L.J., 20th Symp. (Int.) on Combustion (1984), 789.
29. Kiefer, J.H., Mizerka, L.J., Patel, M.R., and Wei, H.C., J. Phys. Chem., 89, (1985), 2013.
30. Kiefer, J.H., Mitchell, K.I., Kern, R.D., and Yong, J.N., manuscript submitted to J. Phys. Chem.
31. Tanzawa, T. and Gardiner, W.C., J. Phys. Chem., 84, (1980), 236.
32. Kiefer, J.H., Kapsalis, S.A., Al-Alami, M.Z., and Budach, K.A., Combust. Flame, 51, (1983), 79.
33. Colket, M.B., presented at the 21st Symp. (Int.) on Combustion, 1986, in press.
34. Hidaka, Y., Tanaka, K., and Suga, M., Chem. Phys. Lett., 130, (1986), 195.
35. Harris, S.J., and Weiner, A.M., Ann. Rev. Phys. Chem., 36, (1985), 31.

Table 1.

Temperature Decrease During Pyrolyses of Various Fuels

$T_0(K)$	$-\Delta T$ (1.0 msec, 2×10^{17} C atoms cm^{-3})						
	C_3H_4	1,2 C_4H_6	1,3 C_4H_6	C_4H_4	C_2H_2	C_5H_5N	C_7H_8
1500	-	57	88	36	<0.5	25	-
1600	-	114	149	95	1	75	93
1700	41	164	211	150	3	155	162
1800	110	206	268	186	6	235	236
1900	168	239	316	205	10	310	311
2000	206	269	354	208	14	375	379
2100	233	300	378	209	18	415	433
2200	249	325	393	210	23	433	462
2300	258	340	400	212	29	433	471
2400	264	349	402	212	33	433	508

Figure 1

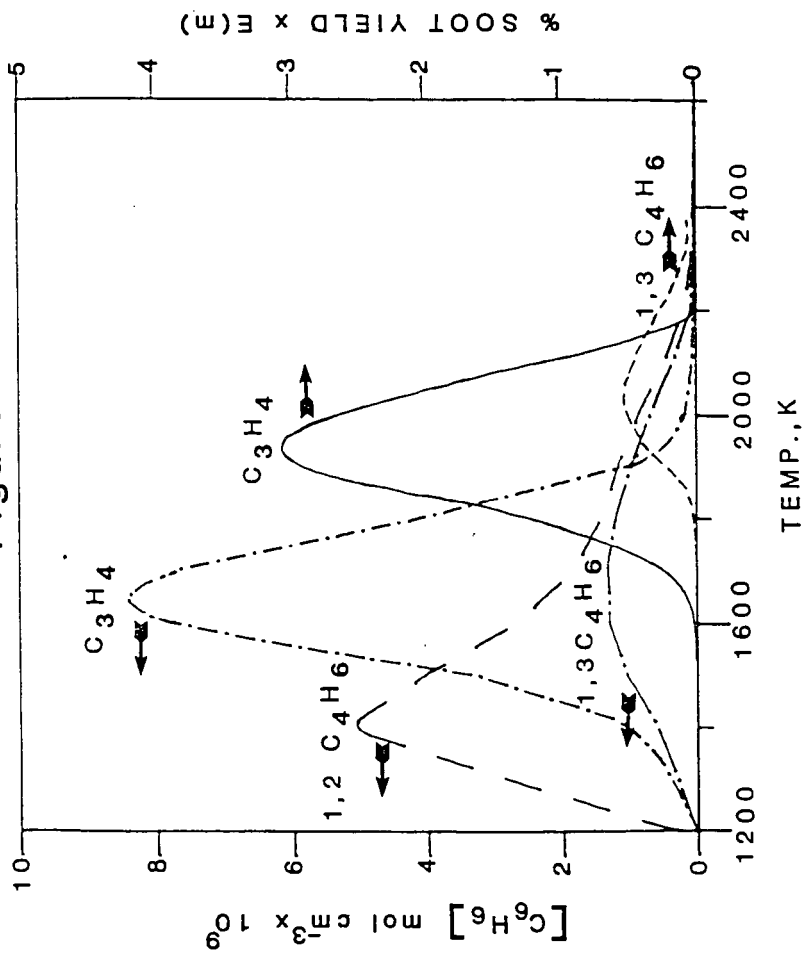


Figure 2

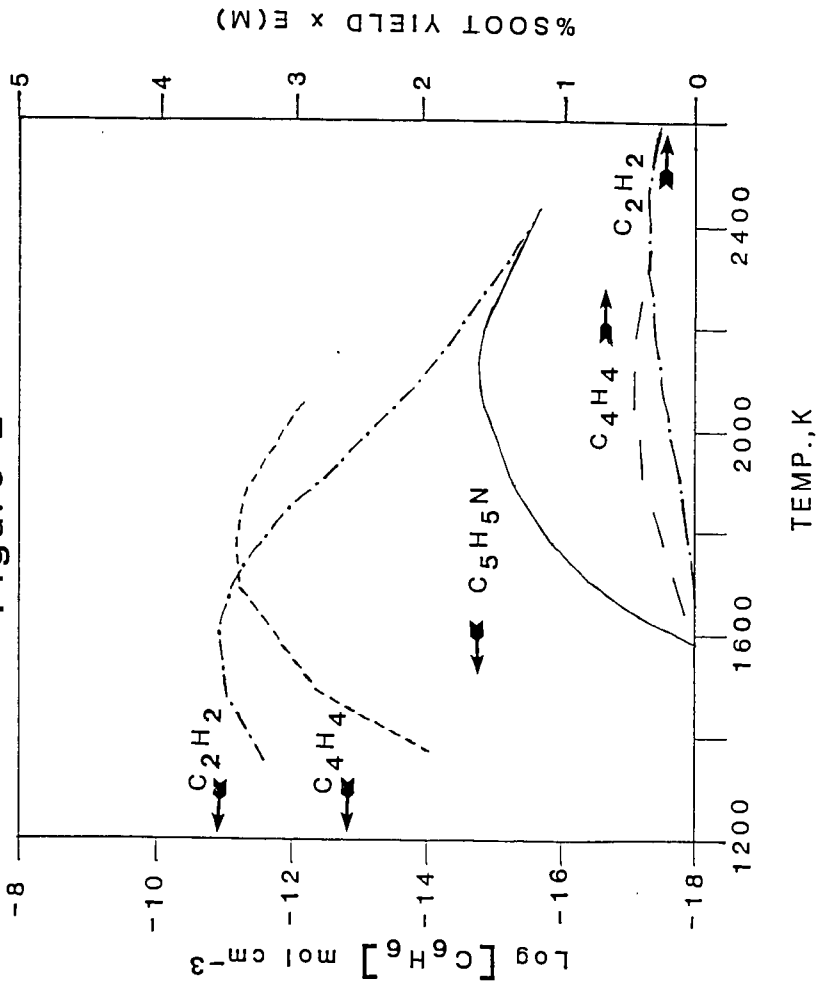


Figure 3
3.7% Acetylene

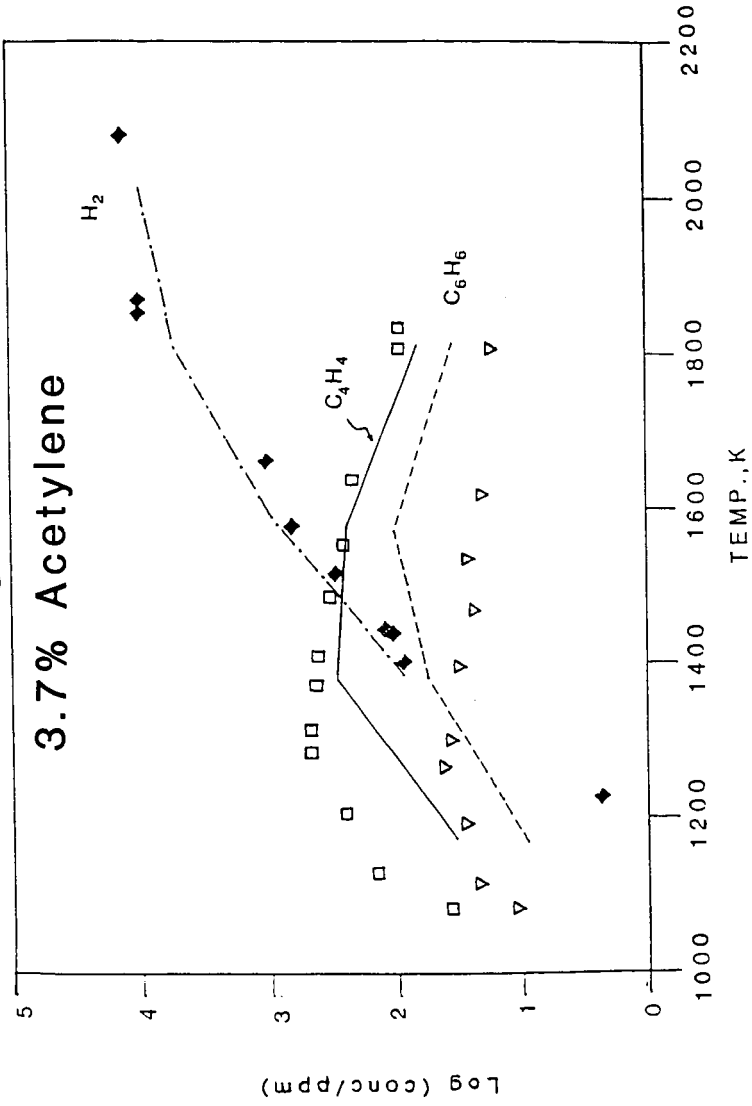


Figure 4

